

See discussions, stats, and author profiles for this publication at:  
<https://www.researchgate.net/publication/235644628>

# Mechanical and thermal properties of hot pressed neodymium-substituted britholite $\text{Ca}_9\text{Nd}(\text{PO}_4)_5(\text{SiO}_4)_2\text{F}_2$

ARTICLE *in* MATERIALS LETTERS · JULY 2003

Impact Factor: 2.49 · DOI: 10.1016/S0167-577X(03)00120-4

---

CITATIONS

11

---

READS

48

4 AUTHORS, INCLUDING:



**Damien Bregiroux**

Pierre and Marie Curie University - Pari...

41 PUBLICATIONS 393 CITATIONS

SEE PROFILE



**Didier Bernache-Assollant**

École Nationale Supérieure des Mines...

67 PUBLICATIONS 1,874 CITATIONS

SEE PROFILE



ELSEVIER

Available online at [www.sciencedirect.com](http://www.sciencedirect.com)

SCIENCE @ DIRECT®

Materials Letters 57 (2003) 3526–3531

**MATERIALS  
LETTERS**

[www.elsevier.com/locate/matlet](http://www.elsevier.com/locate/matlet)

# Mechanical and thermal properties of hot pressed neodymium-substituted britholite $\text{Ca}_9\text{Nd}(\text{PO}_4)_5(\text{SiO}_4)\text{F}_2$

Damien Brégeroux<sup>a,b</sup>, Fabienne Audubert<sup>b</sup>, Eric Champion<sup>a</sup>,  
Didier Bernache-Assollant<sup>a,\*</sup>

<sup>a</sup> *Science des Procédés Céramiques et des Traitements de Surfaces, UMR CNRS 6638, 123 Avenue Albert Thomas, 87060 Limoges Cedex, France*

<sup>b</sup> *CEA Cadarache, DEN/DED/SEP/LCC, 13108 Saint Paul Lez Durance, France*

Received 21 November 2002; accepted 17 January 2003

## Abstract

Neodymium-substituted britholite, a phosphate–silicate apatite  $\text{Ca}_9\text{Nd}(\text{PO}_4)_5(\text{SiO}_4)\text{F}_2$ , is considered as a potential host matrix for specific immobilization of radionuclides. Complementary investigations have been carried out to complete the database concerning this compound. The aim was to establish mechanical and thermal properties of dense britholite. Hot pressing was used to nearly fully densify the material. Low values of mechanical properties were found: 0.75 MPa m<sup>1/2</sup> for the fracture toughness and 95 MPa for the flexural strength. The Young's modulus and the Poisson's ratio were 108 GPa and 0.30, respectively. The specific and the thermal conductivity at 298 K were  $C_p = 0.75 \text{ J g}^{-1} \text{ K}^{-1}$  and  $\lambda = 1.15 \text{ W m}^{-1} \text{ K}^{-1}$ . The average coefficient of thermal expansion in the 20–1000 °C temperature range was  $\alpha = 21 \times 10^{-6} \text{ K}^{-1}$ .

© 2003 Elsevier Science B.V. All rights reserved.

**Keywords:** Ceramics; Britholites; Mechanical properties; Elastic properties; Thermal properties

## 1. Introduction

One of the fields of research conducted in the framework of the French law of 30 December 1991 concerning the management of long-lived and high-activity radioactive waste consists in separating the radionuclides to perform their specific immobilization. Thus, it is necessary to optimize adapted host matrices for long-live radionuclides [1,2]. Several types of matrices have been investigated: glasses, ceramics

and composites [3–5]. Geological observations have led scientists to study apatite minerals as nuclear waste matrices [6]. Studies of natural apatites from the fossil nuclear reactor of Oklo (Gabon) showed that these compounds can support a very high dose of external and internal alpha irradiation. They can also incorporate a large amount of actinides, rare-earth elements and halogens [7]. Neodymium-substituted britholite, a phosphate–silicate apatite  $\text{Ca}_9\text{Nd}(\text{PO}_4)_5(\text{SiO}_4)\text{F}_2$ , is considered as a potential host matrix for the specific immobilization of actinides (americium, curium and neptunium). Neodymium is used to simulate the trivalent actinides because of its similar chemical properties. The optimal formula  $\text{Ca}_9\text{Nd}(\text{PO}_4)_5(\text{SiO}_4)\text{F}_2$  allows the

\* Corresponding author. Tel.: +33-5-55-45-73-70; fax: +33-5-55-45-75-86.

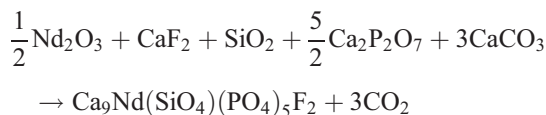
E-mail address: [bernache@unilim.fr](mailto:bernache@unilim.fr) (D. Bernache-Assollant).

incorporation of 10 wt.% of actinides with a low phosphate/silicate ratio. It has been showed that britholites with one silicate and two fluoride ions per cell were not affected by metamictisation (disruption of the crystal lattice) due to alpha particles and recoil nuclei, despite the intense internal ( $3$  to  $10 \times 10^{22} \alpha \text{ m}^{-3}$ ) and external ( $10^{21} \text{ n cm}^{-2}$ ) irradiation doses [8]. More, the apatitic structure can anneal the defects created by self-irradiation, even at low temperature. Another remarkable property, which makes britholites very interesting for nuclear waste storage, is that they have a low solubility that decreases when the temperature increases. Nevertheless, complementary investigations are necessary to complete the database of this compound, notably concerning the mechanical and thermal properties that are of importance for the expected applications. On these bases, this paper is concerned with the sintering by hot pressing of the neodymium-substituted britholite and with the determination of some of its mechanical (flexural strength, fracture toughness and elastic moduli) and thermal (specific heat and coefficient of thermal expansion) properties.

## 2. Materials and methods

### 2.1. Preparation of materials

The neodymium-substituted britholite powder was synthesized by high temperature solid–solid reaction of a  $\text{Nd}_2\text{O}_3/\text{CaF}_2/\text{SiO}_2/\text{Ca}_2\text{P}_2\text{O}_7/\text{CaCO}_3$  mixture [7,9,10] according to the following reaction:



The reaction was completed at  $1400^\circ\text{C}$  for 6 h in air. The britholite structure of the synthesized powder was confirmed by X-ray diffractometry (Fig. 1) and the chemical composition was measured by electron microprobe analysis (Table 1). The powder was ground using attrition milling for 4 h in order to reduce the grain size, which decreases the sintering temperature. The specific surface area of the ground powder, measured according to the BET method (8 points,  $\text{N}_2$ , analyzer Micromeritics ASAP2010, USA), was  $13 \text{ m}^2$

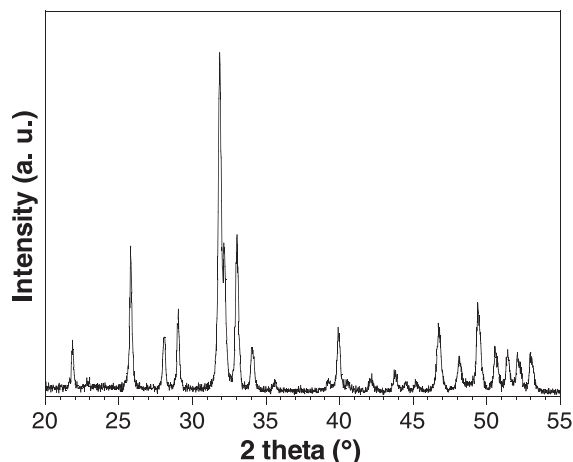


Fig. 1. X-ray diffraction pattern of the as synthesized britholite powder.

$\text{g}^{-1}$ . Blocks of 30 mm in diameter were densified by hot pressing (LPA equipment, France) for 1–4 h at different temperatures in an argon atmosphere and under a compressive stress of 30 MPa. The compressive load was removed at the end of the holding time at high temperature. The heating rate was  $20^\circ\text{C min}^{-1}$  and the cooling rate was  $10^\circ\text{C min}^{-1}$ . This technique was chosen in order to densify the materials at lower temperature than natural sintering.

### 2.2. Characterization of materials

The relative density of sintered samples was measured by the Archimedeian method in water. The theoretical density of the Nd–britholite, calculated from its lattice parameters, was 3.48. The microstructure of the materials was revealed on mirror polished surfaces by thermal etching and it was observed using scanning electron microscopy (SEM-Philips XL30, North-Holland). The grain size distribution was determined from SEM images using a commercial software (Graftek, OptiLabTM/Pro-F2.6.1., Alliance Vision, France).

The Young's modulus ( $E$ ) and the Poisson's ratio ( $\nu$ ) were measured according to the impulse excitation technique using a GrindoSonic system (Lemmens, Germany) on hot pressed pellets of 30 mm in diameter. Hot pressed blocks were cut into  $25 \times 4 \times 4 \text{ mm}^3$  bars using a diamond saw. Then, the bars were polished with a  $3 \mu\text{m}$  diamond paste and their flexural strength ( $\sigma_f$ ) was measured by three-point bending

Table 1  
Electron microprobe analysis of the powder

	Wt.% Ca	Wt.% Nd	Wt.% P	Wt.% Si	Wt.% F
Measured	32.63	13.08	13.66	2.41	2.60
Theory	32.40	13.00	13.90	2.50	3.40

using a 20 mm span and a crosshead speed of  $0.2 \text{ mm min}^{-1}$ . The fracture toughness ( $K_{IC}$ ) was measured using the Vickers indentation technique (durometer Zwick 3212, Germany) on polished samples. A 4.905 N load was applied during 10 s.  $K_{IC}$  values were calculated according to the following equation derived from the model proposed by Evans and Charles [11]:

$$K_{IC} = 0.0824 \frac{N}{c^{3/2}}$$

where  $N$  is the indentation load and  $c$  is the length of the induced radial crack.

The coefficient of thermal expansion ( $\alpha$ ) was determined from dilatometry (Setaram TMA 92, France) on a 8 mm diameter and 3 mm high pellet initially densified up to 98.7% of the theoretical density by hot pressing at  $1250^\circ\text{C}$  during 1 h under a 30 MPa compressive stress. The sample was heated up to  $1000^\circ\text{C}$  at the rate of  $2^\circ\text{C min}^{-1}$  and an average value of the linear coefficient of thermal expansion was calculated in the  $20\text{--}1000^\circ\text{C}$  temperature range. The specific heat measurements were performed on ground powders using a calorimeter Calvet (Setaram C80, France). The measurements were done from 30 up to  $296^\circ\text{C}$  with a holding time of 3 h at the ambient temperature, 1 h at  $30^\circ\text{C}$  and 1 h at  $296^\circ\text{C}$  before cooling. The heating and cooling rates were  $0.2^\circ\text{C min}^{-1}$ . The thermal conductivity was determined from the thermal diffusivity measured on a 3-mm-thick pellet having a bulk density of  $3.34 \text{ g cm}^{-3}$ . The flash laser method was used and the thermal diffusivity was calculated using the Degiovanni's model.

### 3. Results and discussion

#### 3.1. Hot pressing

The relative density of materials hot pressed for 1 h at different temperatures is given in Fig. 2. A minimum of  $1250^\circ\text{C}$  was required to reach a relative density of at least 98% of the theoretical value. The densification

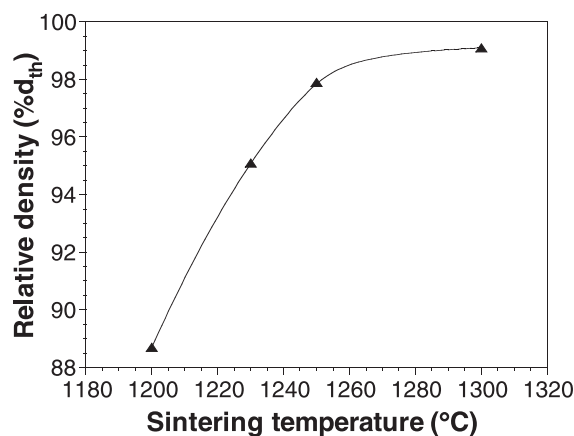


Fig. 2. Relative density of materials versus the temperature of hot pressing (1 h, 30 MPa).

versus time for the hot pressing cycle at this temperature of  $1250^\circ\text{C}$  is plotted in Fig. 3. The curve could be splitted in two parts. In a first time, the relative density decreased because of the thermal expansion. Then, from about 50 min, which corresponded to a temperature close to  $1000^\circ\text{C}$ , the densification began. The highest relative density was reached at the end of the holding time at high temperature.

The microstructure of the hot pressed blocks was homogeneous (Fig. 4). No important grain growth was observed when the holding time increased as shown on the example of Fig. 5. The average grain size remained almost constant at about  $1.2 \mu\text{m}$ . It can be hypothesized that the temperature is not high enough to activate the grain growth process. Another explanation could be a pinning of grain boundaries due

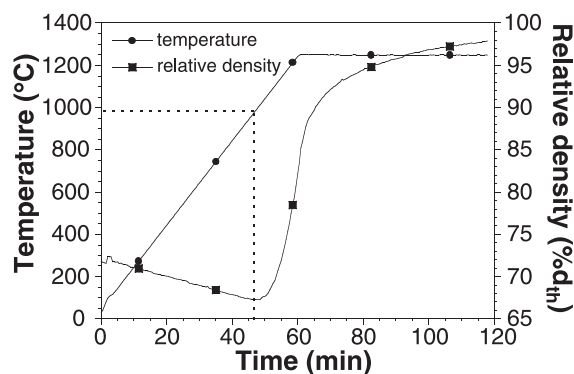


Fig. 3. Development of the relative density of the material during the hot pressing cycle ( $1250^\circ\text{C}$ , 30 MPa, 1 h).

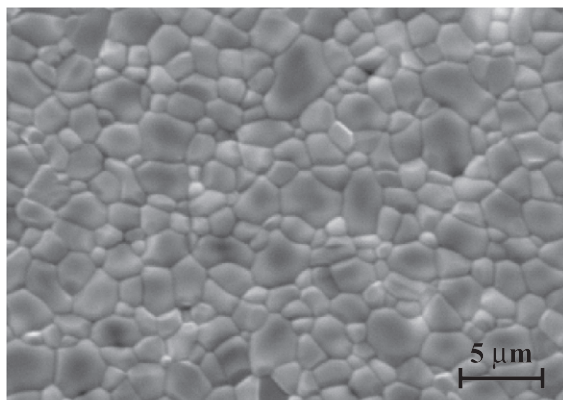


Fig. 4. SEM micrograph of a hot pressed material (1250 °C, 1 h, 30 MPa).

to the presence of impurities located at these grain boundaries, which would impede their displacement. The grain size distributions (Fig. 6) can bring more information. They showed that the size of the coarsest grains increased with the holding time at high temperature during hot pressing, even if the mean diameter remained almost constant. Finally, a light broadening of the grain size distribution occurred with the increasing of the hot pressing time.

### 3.2. Thermal properties

The linear thermal expansion of the neodymium-substituted britholite versus the temperature is plotted

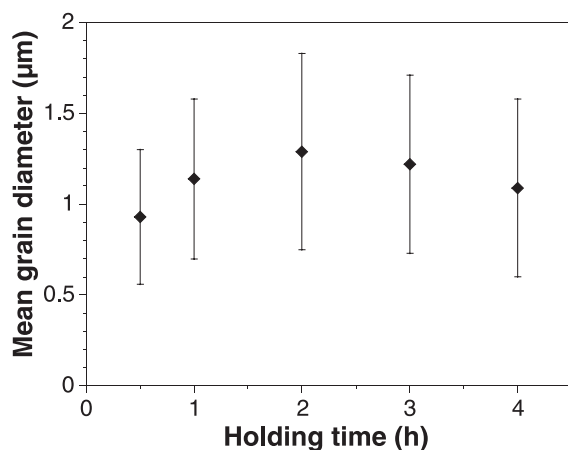


Fig. 5. Mean grain diameter versus the holding time of hot pressing at 1300 °C under 30 MPa.

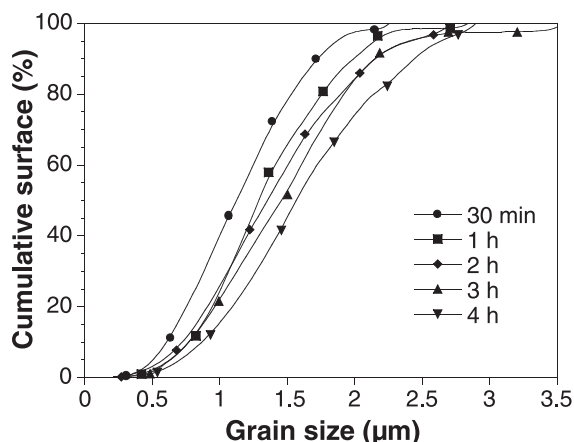


Fig. 6. Grain size distribution of materials hot pressed at 1300 °C under 30 MPa for various holding times.

in Fig. 7. The linear coefficient of thermal expansion was almost constant in the 20–1000 °C temperature range. The average value calculated in the 20–1000 °C temperature range was  $\alpha = 21 \times 10^{-6} \text{ K}^{-1}$ . It is important to note that the measurement was performed on a polycrystalline sample. Consequently, this value is an average of the coefficients of thermal expansion of the *a* and *c* axes of the hexagonal cell of the Nd–britholite crystals. Compared with other ceramic materials, this coefficient of thermal expansion is very high. For example, the average value for calcium phosphate hydroxyapatite, which is known to

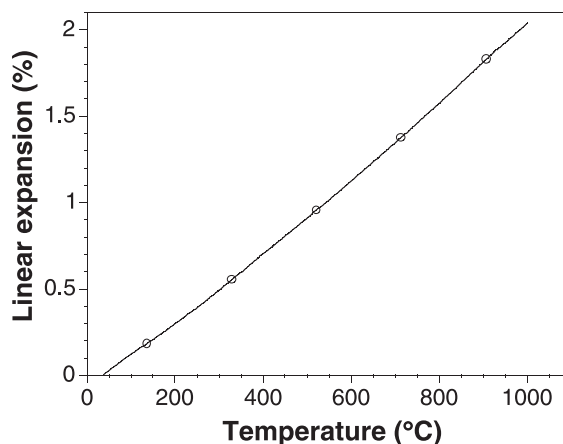


Fig. 7. Linear thermal expansion of the Nd-substituted britholite.

have a high coefficient of thermal expansion, is  $16 \times 10^{-6} \text{ K}^{-1}$  [12].

The variation of the specific heat of the material with the temperature (in the 20–296 °C range) corresponded with the following equation:

$$C_p = 0.64 + 3.64 \times 10^{-4} T$$

where  $C_p$  is the specific heat expressed in  $\text{J g}^{-1} \text{ K}^{-1}$  and  $T$  is the temperature expressed in Kelvin. This equation gives a value of  $0.75 \text{ J g}^{-1} \text{ K}^{-1}$  at the ambient temperature ( $T = 298 \text{ K}$ ), which corresponds with  $794 \text{ J mol}^{-1} \text{ K}^{-1}$ . For a comparison, the specific heat is 67.05 for alumina, 455.4 for hollandite and  $193.3 \text{ J mol}^{-1} \text{ K}^{-1}$  for zirconolite [4].

The thermal conductivity at the ambient temperature  $\lambda = 1.15 \text{ W m}^{-1} \text{ K}^{-1}$ . This value is close to those found for other ceramic materials of interest for waste forms such as apatite, zirconolite or monazite whose thermal conductivities are between 0.8 and  $2 \text{ W m}^{-1} \text{ K}^{-1}$  [4,13].

### 3.3. Mechanical properties

The value of the Young's modulus measured on a material densified at 99.4% of the theoretical density was  $E = 108 \text{ GPa}$ , which is close to the sole value that can be found in the literature for britholite (96 GPa) [4]. The Poisson's ratio was  $\nu = 0.30$ . The shear modulus calculated from the values of  $E$  and  $\nu$  was  $G = 41 \text{ GPa}$ .

The flexural strength and the fracture toughness of dense materials are given in Fig. 8. Both character-

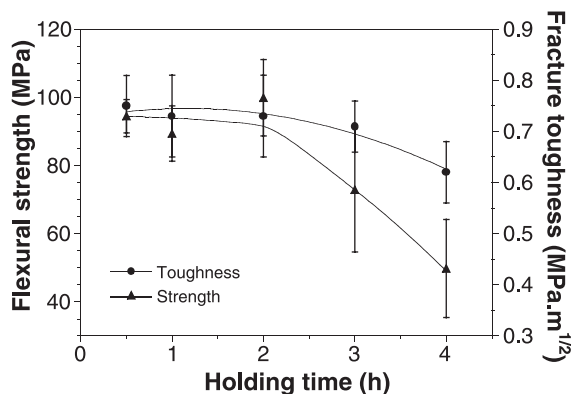


Fig. 8. Flexural strength and fracture toughness of dense materials hot pressed for various times at 1300 °C under 30 MPa.

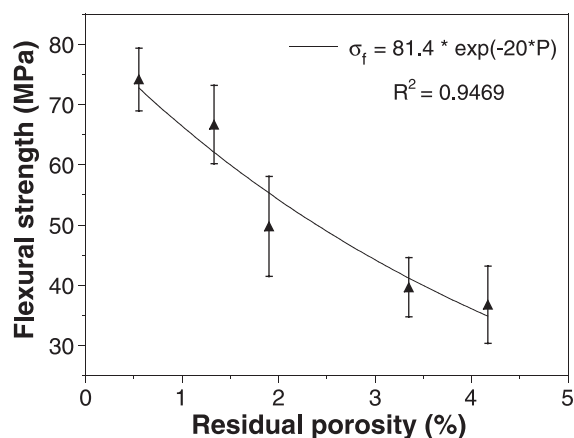


Fig. 9. Flexural strength versus the residual porosity of hot-pressed materials (the line drawing represents Eq. (1) fitted to the experimental data).

istics have similar variations. The maximum values were  $\sigma_r = 95 \pm 5 \text{ MPa}$  and  $K_{IC} = 0.75 \pm 0.05 \text{ MPa m}^{1/2}$  for the materials having the smallest grain size (i.e., materials hot pressed at 1300 °C for less than 2 h). These values are indicative of a highly brittle behavior of this material. The broadening of the grain size distribution with the increasing holding time during hot pressing induced a decrease of the mechanical properties. This is explained by the increase of the size of the coarsest grains that control the failure of dense brittle ceramic materials. For such materials, the fracture strength depends on the grain size according to a law that can be written as follows:

$$\sigma_r = A d^{-a}$$

where  $d$  is the grain size,  $A$  and  $a$  are two experimental constants and  $a$  is generally close to 0.5. For the materials having a residual porosity, the mechanical properties are governed by the pores that constitute the critical defects. The fracture strength follows a classical exponential law [14]:

$$\sigma_r = \sigma_0 \exp(-bP) \quad (1)$$

where  $\sigma_0$  is the maximum fracture strength (i.e., the extrapolated strength corresponding with the dense material),  $b$  is a constant and  $P$  is the porosity ratio ( $0 \leq P \leq 1$ ). Eq. (1) fitted to the experimental data (Fig. 9) gave calculated values of  $\sigma_0 = 81.4 \text{ MPa}$  and  $b = 20$ .



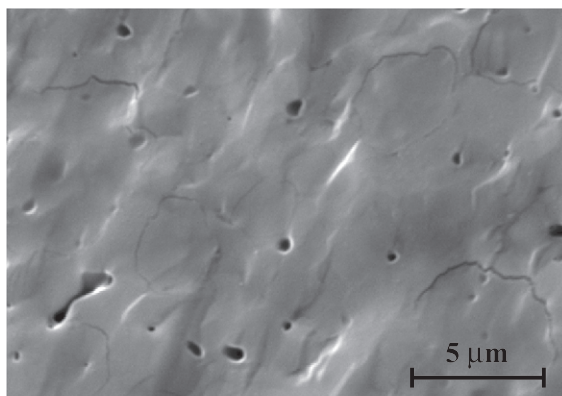


Fig. 10. SEM micrograph of a fracture surface (material hot pressed at 1250 °C, 1 h, 30 MPa).

No result is available in the literature concerning the mechanical characteristics of britholite ceramics. But, for a comparison, the neodymium-substituted apatite has a mechanical behavior close to that of another well-known apatitic compound: calcium phosphate hydroxyapatite  $\text{Ca}_{10}(\text{PO}_4)_6(\text{OH})_2$  [15].

From the previous results, it was possible to determine the first parameter of thermal shock resistance, called  $R$ , which represents the theoretical instantaneous difference of temperature required to provoke a cracking of the material:

$$R = \frac{\sigma_r(1 - \nu)}{\alpha E}$$

For Nd-substituted britholite,  $R$  is equal to about 30 K. It means that this material is not thermal shock resistant since it cannot support a temperature variation higher than 30 K without appearance of cracks.

SEM examination of the fracture surfaces (Fig. 10) revealed that the crack propagation seemed to occur according to a transgranular mode of failure. This observation allows to explain the low level of fracture toughness. In a transgranular mode of failure for brittle materials, the cracks do not follow the grain boundaries so that there is no crack deflection along them. In that case, energy dissipation during crack propagation remains very low.

#### 4. Conclusion

The mechanical and thermal properties of neodymium-substituted britholite, a potential host matrix for actinides immobilization, were measured in order to complete its database. From the mechanical point of view, this ceramic material exhibited a brittle behavior associated with a low fracture toughness (below 1 MPa m<sup>1/2</sup>), viz. a low resistance to crack propagation. The thermal properties are characterized by a high coefficient of thermal expansion, which, in association with the mechanical characteristics, induces a low resistance to thermal shocks. Nevertheless, the high specific heat of the Nd–britholite constitutes an advantage in order to limit the temperature rising due to the thermal effects associated with the nuclear disintegration of radionuclides.

#### References

- [1] R.C. Ewing, W. Lutze, MRS Bull. 19 (1994) 16.
- [2] C. Guy, F. Audubert, J.-E. Lartigue, C. Latrille, T. Advocat, C. Fillet, C.R. Phys. 3 (2002) 827.
- [3] R.C. Ewing, W.J. Weber, F.W. Clinard, Prog. Nucl. Energy 29 (1995) 63.
- [4] P. Trocellier, Ann. Chim. Sci. Mat. 25 (2000) 321.
- [5] P. Trocellier, Ann. Chim. Sci. Mat. 26 (2001) 113.
- [6] J. Carpena, F. Audubert, D. Bernache-Assolant, L. Boyer, B. Donazzon, J.-L. Lacout, N. Senamaud, in: I.G. McKinley, C. McCombie (Eds.), Scientific Basis for Nuclear Waste Management, vol. XXI, Materials Research Society, Warrendale, PA, 1998, p. 543.
- [7] J. Carpena, L. Boyer, M. Fialin, J.-R. Kiénast, J.-L. Lacout, C.R. Acad. Sci. Paris 333 (2001) 373.
- [8] V. Sere, PhD Thesis, University of Paris VII, Paris (1996).
- [9] L. Boyer, J. Carpena, J.L. Lacout, Solid State Ionics 95 (1997) 121.
- [10] J. Carpena, L. Boyer, J.-L. Lacout, CEA Patent No. 98 11334 (1998).
- [11] A.G. Evans, E.A. Charles, J. Am. Ceram. Soc. 59 (1976) 371.
- [12] G.R. Fischer, P. Bardhan, J.E. Geiger, J. Mater. Sci. Lett. 2 (1983) 577.
- [13] M. Uno, M. Shinohara, K. Kurosaki, S. Yamanaka, J. Nucl. Mater. 294 (2001) 119.
- [14] E. Ryshkewitch, J. Am. Ceram. Soc. 36 (1953) 65.
- [15] R. Halouani, D. Bernache-Assolant, E. Champion, A. Ababou, J. Mater. Sci., Mater. Med. 5 (1994) 563.